Characterization of the *Fusarium circinatum* biofilm environmental response role

Francinah M. Ratsoma[1], Nthabiseng Z. Mokoena[1], Quentin C. Santana[1,2], Brenda D. Wingfield[1], Emma T. Steenkamp[1], Thabiso E. Motaung[1]

[1]Department of Biochemistry, Genetics, and Microbiology, Forestry and Agricultural Biotechnology Institute (FABI), University of Pretoria, Pretoria, South Africa

[2]Agricultural Research Council (ARC) Biotechnology Platform, Private Bag X5 Onderstepoort, Pretoria, South Africa

*Correspondence: Thabiso E. Motaung, Department of Biochemistry, Genetics, and Microbiology, Forestry and Agricultural Biotechnology Institute (FABI), University of Pretoria, Hatfield 0083, Pretoria, South Africa. Email: thabiso.motaung@up.ac.za

Funding information

South African National Research Foundation (NRF), Grant/Award Number: 129580; South African National Department of Science and Innovation-NRF Centers of Excellence program and South African Research Chairs Initiative, Grant/Award Number: 98353.

Abstract

The capacity to form biofilms is a common trait among many microorganisms present on Earth. In this study, we demonstrate for the first time that the fatal pine pitch canker agent, *Fusarium circinatum*, can lead a biofilm-like lifestyle with aggregated hyphal bundles wrapped in extracellular matrix (ECM). Our research shows *F. circinatum*'s ability to adapt to environmental changes by assuming a biofilm-like lifestyle. This was demonstrated by varying metabolic activities exhibited by the biofilms in response to factors like temperature and pH. Further analysis revealed that while planktonic cells produced small amounts of ECM per unit of the biomass, heat- and azole-exposed biofilms produced significantly more ECM than nonexposed biofilms, further demonstrating the adaptability of *F. circinatum* to changing environments. The increased synthesis of ECM triggered by these abiotic factors highlights the link between ECM production in biofilm and resistance to abiotic stress. This suggests that ECM-mediated response may be one of the key survival strategies of *F. circinatum* biofilms in response to changing environments. Interestingly, azole exposure also led to biofilms that were resistant to DNase, which typically uncouples biofilms by penetrating the biofilm and degrading its extracellular DNA; we propose that DNases were likely hindered from reaching target cells by the ECM barricade. The interplay between antifungal treatment and DNase enzyme suggests a complex relationship between eDNA, ECM, and antifungal agents in *F. circinatum* biofilms. Therefore, our results show how a phytopathogen's sessile (biofilm) lifestyle could influence its response to the surrounding environment.

Keywords: abiotic stress, antifungals, biofilms, DNase, extracellular DNA, Fusarium circinatum

Abbreviations

CAAF - Concanavalin A-Alexa Fluor 488 conjugate; ECM - extracellular matrix; eDNA - extracellular DNA; EDTA - ethylenediaminetetraacetic acid; EPS - extracellular polymeric substances; FUN-1 - 2-chloro-4-(2,3-dihydro-3-methyl-(benzo-1,3-thiazol-2-yl)-methylidene)-1phenylquinolinium iodide; HMDS - hexamethyldisilazane; PBS - phosphate buffered saline; PDA - potato dextrose agar; PDB - potato dextrose broth; SEM - scanning electron microscopy; XTT - 2,3-bis(2-methoxy-4-nitro-5-sulfophenyl)-2H-tetrazolium-5-carboxanilide

1 INTRODUCTION

The capacity to form a biofilm is a fundamental survival strategy used by microorganisms, including bacteria, archaea, fungi, and even some microalgae. A biofilm is a microbial community of sessile cells attached to biotic and/or abiotic surfaces while embedding itself in a slimy heterogenous extracellular matrix (ECM) [1, 2]. ECM is mainly comprised of water and extracellular polymeric substances (EPS) such as carbohydrates, extracellular DNA (eDNA), lipids, and proteins [3, 4]. Because ECM is typically found between biofilm forming microbial cells, gluing them together [4, 5], it determines the three-dimensional architecture of biofilms [6]. ECM also contributes to various additional properties differentiating biofilms from planktonic or free-living cells [7, 8]. Among others, these include enhanced tolerance to environmental changes (e.g., in salinity and pH) and harmful substances such as antimicrobial compounds. Although biofilm formation has not been widely studied in filamentous fungi, it occurs through a succession of phases involving reversible and irreversible attachment, production of adhesive substances, microcolony formation, development, and maturation to an ECM-enclosed structure from which fruiting bodies ultimately release spores for dispersal [9-11].

The distinctive chemical and physical makeup of plant tissues presents both a challenging and desirable ecosystem for microbial colonists to form biofilms [8]. Indeed, ECM production, in association with plants and their biofilm-forming colonists, has been reported by several studies [12]. For example, phytopathogenic bacteria, such as *Pseudomonas syringae* pv. *phaseolicola* and *Curtobacterium flaccumfaciens* pv. *flaccumfaciens*, form biofilms on the surfaces of dried bean seeds and sprouts that are accompanied by ECM production [12]. In addition, several vascular pathogens (e.g., *Xylella fastidiosa* and *Ralstonia solanacearum*) clog their hosts' xylem vessels via ECM-embedded cells [13, 14]. *In planta* studies of fungal biofilms are rare, but it has been shown that *Aspergillus niger* infection in onion bulbs is associated with biofilms embedded within the ECM [15]. In a recent paper by [16], biofilm-like structures formed by *Zymoseptoria tritici* were found to colonize the leaf surface of susceptible and resistant wheat hosts, suggesting that biofilms may have a role to play in disease development. Also, a range of plant-associated fungal pathogens produce biofilms under laboratory conditions [17, 18], but very little is known about how biofilm formation, particularly ECM production, affects plant disease.

Here, we investigated whether the filamentous fungus, *Fusarium circinatum*, is capable of biofilm production. This species is often referred to as the pitch canker fungus and is notorious for causing resinous cankers on the trunks, branches, and roots of trees, and root rot of seedlings in susceptible *Pinus* species [19-21]. The fungus occurs in almost all regions where these plants are cultivated commercially, and in some areas, it also threatens natural *Pinus* stands [22, 23]. The possibility that *F. circinatum* may live in a biofilm-like environment, which may form part of its virulence profile, has not been investigated. This is despite the fact that other

economically important plant-associated members of the genus (e.g., *Fusarium graminearum, Fusarium verticillioides*, and *Fusarium oxysporum* f. sp. *cucumerinum*) form biofilms that are primarily distinguished by the production of ECM [18, 24, 25].

Our study had two aims. First, we explored the ability of *F. circinatum* to form surface-attached cultures, embedded within self-produced gelatinous matrixes similar to those exemplifying biofilms. Second, we examined how these structures, as well as their composition and activity, might be influenced by various abiotic factors. To achieve these aims, we used a well-known pathogenic strain of the fungus [26], for which a wealth of biological information has been accumulated over the last two decades (e.g., [27-30]). By making use of an array of laboratory and microscope-based approaches, we demonstrate that *F. circinatum* produces biofilms in vitro, and that their formation is significantly impacted by pH, temperature, and osmotic stress, suggesting that biofilm might be a type of adaptive strategy employed by *F. circinatum* under certain environmental conditions. We also show enhanced production of ECM in the presence azole fungicides and DNase, which implies that azole-induced ECM production provided protection against eDNA degradation. This is the first study to link ECM and eDNA to an antifungal response in phytopathogenic fungi, thus greatly improving the knowledge of *F. circinatum* biology and revealing a previously unrecognized antifungal resistance strategy.

2 MATERIALS AND METHODS

2.1 Growth conditions

Isolate FSP34 (CMW350) of *F. circinatum* was obtained from the culture collection of the Forestry and Agricultural Biotechnology Institute (FABI), University of Pretoria, South Africa. For routinely growing the fungus, it was cultured on potato dextrose agar (PDA) (Merck) for 7 days in the dark at 25°C. When growing the fungus in liquid medium, we used dextrose broth (PDB) containing 6 g/L of Difco™ (Thermo Fisher Scientific Inc.) dehydrated powder. To obtain conidial cells, the agar plates cultures were flooded with 2 mL of 0.2 M phosphate-buffered saline (PBS; 10 mM NaH_2PO_4, 10 mM Na_2HPO_4, 150 mM NaCl, pH 7.2). Conidia were counted in a Neubauer chamber and concentrations adjusted before use in downstream analyses.

2.2 In vitro biofilm formation and visualization

To assess whether isolate FSP34 could form biofilms, 20 µL of a conidial suspension (2×10^5 spores/mL) was added to 10 mL of PDB in sterile 65 mm petri dishes (ChemLab) and incubated statically at room temperature (RT) for 7 days. Biofilm formation was also tracked over time according to Mowat et al. [31], with slight modifications. Briefly, conidial suspensions in PDB (2×10^5 spores/mL) were incubated at RT for 24, 48, 72 h, and 7 days without shaking to allow conidia to settle and adhere to the bottom of chamber slides (Nunc Lab-Tek II Chamber Slide System; Thermo Fisher Scientific Inc.).

At the end of the incubation period, the broth was removed and the slide rinsed with distilled water to remove non-adhering cells. Metabolic activity of the biomass attached to the slides was then appraised using Invitrogen's 2-chloro-4-(2,3-dihydro-3-methyl-(benzo-1,3-thiazol-2-yl)-methylidene)-1phenylquinolinium iodide (FUN-1; Thermo Fisher Scientific Inc.), while ECM production was assessed with the cell wall polysaccharide-binding fluorescent dye concanavalin A-Alexa Fluor 488 conjugate (CAAF; Thermo Fisher Scientific Inc.). This was achieved by flooding the rinsed slide with 200 µL of a solution containing 25 µg/mL of CAAF

and 25 µg/mL of FUN-1 The fluorescent dyes were discarded and the slides were rinsed with PBS and assessed using ZEISS confocal laser scanning microscope 880, with excitation at 488/543 nm and emission at 505/560 nm for FUN1 and CAAF, respectively, using the 63× oil immersion lens (Laboratory for Microscopy and Microanalysis at University of Pretoria).

Biofilms were subjected to scanning electron microscopy (SEM) for structural analysis. For this purpose, sterile 65 mm petri dishes containing glass coverslips and 200 mL PDB were inoculated with 20 µL conidial cells (to a final concentration of 2×10^5 cells/mL) and statically incubated at RT for 7 days. Glass slides were then removed and flooded and rinsed with PBS before adding the pre-fixative solution containing 1 mL of 2.5% (v/v) glutaraldehyde (Merck)/formaldehyde (Merck). After another PBS rinse, biofilms were fixed with 1% osmium tetroxide for 1 h. Following a final PBS rinse, the fixed biofilms were dehydrated sequentially using a series of graded ethanol (i.e., 15 min rinses each in 1 mL of ethanol at concentrations of 30%, 50%, 70%, 90%, and three rinses in absolute ethanol). The dehydrated samples were then treated with a 50:50 mixture of hexamethyldisilazane (HMDS) and absolute ethanol for 1 h, followed by a treatment with HMDS only, after which they were left to dry overnight. The glass slides were mounted on rectangle aluminum stubs and carbon coated for 15 min using Quorum Q150T ES sputter coater (Quorumtech). The stubs were observed in a JEOL JSM 6490LV scanning electron microscope (GenTech Scientific Inc.).

2.3 Biofilm biomass, metabolic activity, eDNA, and ECM production

For quantifying the *F. circinatum* biofilm biomass, we used the basic dye crystal violet (Merck) to stain biofilm cells and their surrounding biofilm matrix [32]. The stained biofilm was quantified as described previously [33, 34]. To achieve this, biofilm was established by inoculating a 96-well flat-bottom polystyrene plate (Thermo Fisher Scientific Inc.) containing 200 µL of PDB with FSP34 conidia to a final concentration of 2×10^5 cells/mL and then incubating it statically for 7 days at RT. For comparative purposes, another plate was prepared in the same way, but incubated with shaking to assess biomass production for planktonic cells. Biofilms were then rinsed with PBS to remove loose cells while plates containing planktonic cells were centrifuged (10 000×*g* for 10 min at 4°C) and the supernatants discarded. In both cases, cells were fixed with 99% methanol for 15 min, after which the methanol was removed and plates air-dried for 5 min. Fungal biomass in each well was stained with 0.4% (w/v) crystal violet dissolved in absolute ethanol. Following incubation at RT for 30 min, samples were rinsed twice with PBS, after which the biomass in each well was decolorized by incubation at RT for 5 min in 200 µL absolute ethanol. We then recorded the absorbance of the samples at 540 nm using a microplate reader (SpectraMax® Paradigm® Multimode Detection Platform; Molecular Devices LLC).

Metabolic activity was assessed using the Roche Cell Proliferation Kit II (Merck), which utilizes a colorimetric assay based on reduction of the tetrazolium salt XTT (2,3-bis(2-methoxy-4-nitro-5-sulfophenyl)-*2H*-tetrazolium-5-carboxanilide) [35]. Assays were performed on biofilm grown for 72 h and 7 days in 96-well flat-bottom polystyrene plates, as described above, while 5 mL of planktonic cells were shaken in 50 mL Erlenmeyer flasks for 72 h and 7 days, after which 100 µL were transferred to the 96-well plate on the day of analysis. After removal of excess broth and rinsing with PBS, metabolic activity was evaluated with the kit. Following incubation in the presence of the XTT labeling mixture at 37°C in the dark for 3 h, colorimetric changes were measured at 492 nm using a microplate reader.

For ECM analysis, 7-day-old biofilms and planktonic cultures were prepared in 96-well flat-bottom polystyrene plate as described above. ECM production was assayed in both cell types according to Choi et al. [36] with slight modifications [37]. Then, nonfixed biofilms were stained with 200 µL of 0.1% (w/v) of basic fuchsin (Merck), which binds to the polysaccharides of the biofilm, for 5 min at RT. The wells were then washed with PBS until the supernatants were clear. The ECM was decolorized with 200 µL absolute ethanol and measured at 530 nm using a microplate reader.

We investigated whether eDNA might contribute to the stabilization of ECM in *F. circinatum* biofilm, as have been shown for other fungal biofilms [38]. To do this, a 7-day-old biofilm grown as described above was prepared and washed with PBS and treated with 0.2 M EDTA (ethylenediaminetetraacetic acid) (pH 8) to extract the ECM. After centrifugation at 10 000×*g*, the supernatant was recovered and filtered using a 0.45-µM Millipore syringe filter (Merck). From this filtrate, we extracted eDNA using Quick-DNA Fungal/Bacterial Kit (Zymo Research). The quantity of eDNA released from the ECM was determined through a fluorescence assay using Invitrogen's DNA binding dye SYBR® Green I (Thermo Fisher Scientific Inc.), as previously described by Rajendran et al. [39]. Briefly, SYBR® Green I was added to the extracted DNA in a black well microtiter plate (Merck Group) at a ratio of 1:1. The levels of eDNA were quantified in a microplate reader at an excitation of 485 nm and an emission of 535 nm. The concentration of eDNA in the sample was extrapolated from a standard curve as previously described [40]. We independently assessed the impact of bovine pancreas DNase 1 (0.5 mg/mL; Merck) on biofilms, by incubating the 72-h and 7-day-old biofilms in the presence of DNase I treatment at RT for 24 h, after which the ECM per biomass were quantified as before.

2.4 Influence of pH, temperature, carbon source, and osmotic stress on biofilm formation

The impact of abiotic factors on biofilm formation was quantified using the XTT reduction assay as described above. For these experiments, 72 h and 7-day-old biofilms and planktonic cultures were prepared in 96-well flat-bottom polystyrene plates as described above, but the following modifications were incorporated. For testing the effect of temperature, the culture was incubated at 4°C, 15°C, 25°C, 30°C, 37°C. For testing the effect of pH, they were incubated at RT in PDB at pH-values 2, 3, 4, 6, 7, and 8 (adjusted with HCl and 10 M NaOH). For testing the effect of osmotic stress, cultures were grown at RT in PDB supplemented with 1 M NaCl and in PDB medium supplemented with 1.5 M sorbitol.

The effect of different sugars on biofilm formation was evaluated according to Peiqian et al. [18]. This involved preparation of RT-grown 72-h and 7-day-old biofilms and planktonic cultures in 96-well flat-bottom polystyrene plates as described above, except that PDB was replaced minimal medium (20 mg/mL thiamine-HCL, 30 mM glucose, 26 mM glycine, 20 mM $MgSO_4\_7H_2O$, and 58.8 mM KH_2PO_4) supplemented with 30 mM of glucose, maltose, and lactose.

The impact of heat shock on preformed biofilms was evaluated using the biomass, ECM, and XTT reduction assays described above. For this purpose, 72-h and 7-day-old-biofilms and planktonic cultures were prepared in PDB at RT in 96-well flat-bottom polystyrene plates. The respective culture types were then subjected to a heat treatment (30 min to 1 h) at 45°C.

2.5 Biofilm response to azole fungicides

We first determined the various concentrations at which two commercially available fungicides inhibited the radial growth on FSP34 on PDA. These fungicides were imazalil (ICA international chemicals) and Tebuconazole (Arysta Lifescience), and were suspended in sterile distilled water and added to PDA post sterilization (50°C) at concentrations 0, 0.1, 1, 10, and 100 mg/L. Mycelial plugs (5 mm), taken from the margins of 7-day-old PDA cultures with the aid of a cork borer, were then placed at the center of the 90 mm Petri plates (with the mycelium facing towards the medium). Six biological replicates were prepared per concentration of the fungicide to which isolates were exposed. The plates were incubated in the dark for 7 days at 25°C. Following growth, colony diameter was recorded with a metric ruler, using the average of two perpendicular measurements. Percentage of inhibition at the different fungicide concentrations was calculated as (B1-B2)/B1 × 100, where B1 is the radial growth of the fungus in the absence of fungicide and B2 the radial growth in the presence of fungicide.

We also evaluated the various concentrations at which the two fungicides affect biofilm formation [41]. This was done by preparing 7-day-old biofilms at RT in PDB that was supplemented with the respective fungicides, at the respective concentrations (0, 0.1, 1, 10, and 100 mg/L). Inhibition percentage was determined using the crystal violet-based biomass assay described above. As negative controls, we used PDB alone, and PDB with fungicides, while our positive control was PDB plus conidia. Percentage inhibition was determined as (C1–C2)/C1 × 100, where C1 is the growth of biofilm in the absence of fungicide and C2 the biofilm growth in the presence of fungicide. From these data, we then determined the concentrations that inhibited 50% (I_{50}) of the growth of the biofilm.

The impact of imazalil and tebuconazole on 72-h and 7-day-old biofilms and planktonic cultures was determined using the relevant I_{50} concentrations. For this purpose, the two culture types were prepared at RT in 96-well flat-bottom polystyrene plates as described above. We then incubated these cultures in the presence of the respective fungicides, overnight at RT. All samples were then subjected to the biomass, ECM and XTT reduction assays described above. To test whether eDNA might influence the fungicidal impact on the biofilm, the experiment was repeated, but before treating the cultures with fungicide, we first incubated them in the presence of 0.5 mg/mL DNase I for 24 h at RT. Heat inactivated (75°C for 15 min) DNase I and biofilms treated with or without fungicide were used as negative controls.

2.6 Reproducibility and statistical analyses

Statistical analyses were performed using GraphPad statistical software (GraphPad 5 Software). Images were captured using the Epson scanner (Epson perfection V700 photo). The means of all obtained data in the assays were compared using one-way analysis of variance (ANOVA) Tukey's simultaneous comparisons or parametric student's *t*-test analysis. All experiments we performed in triplicate unless otherwise stated.

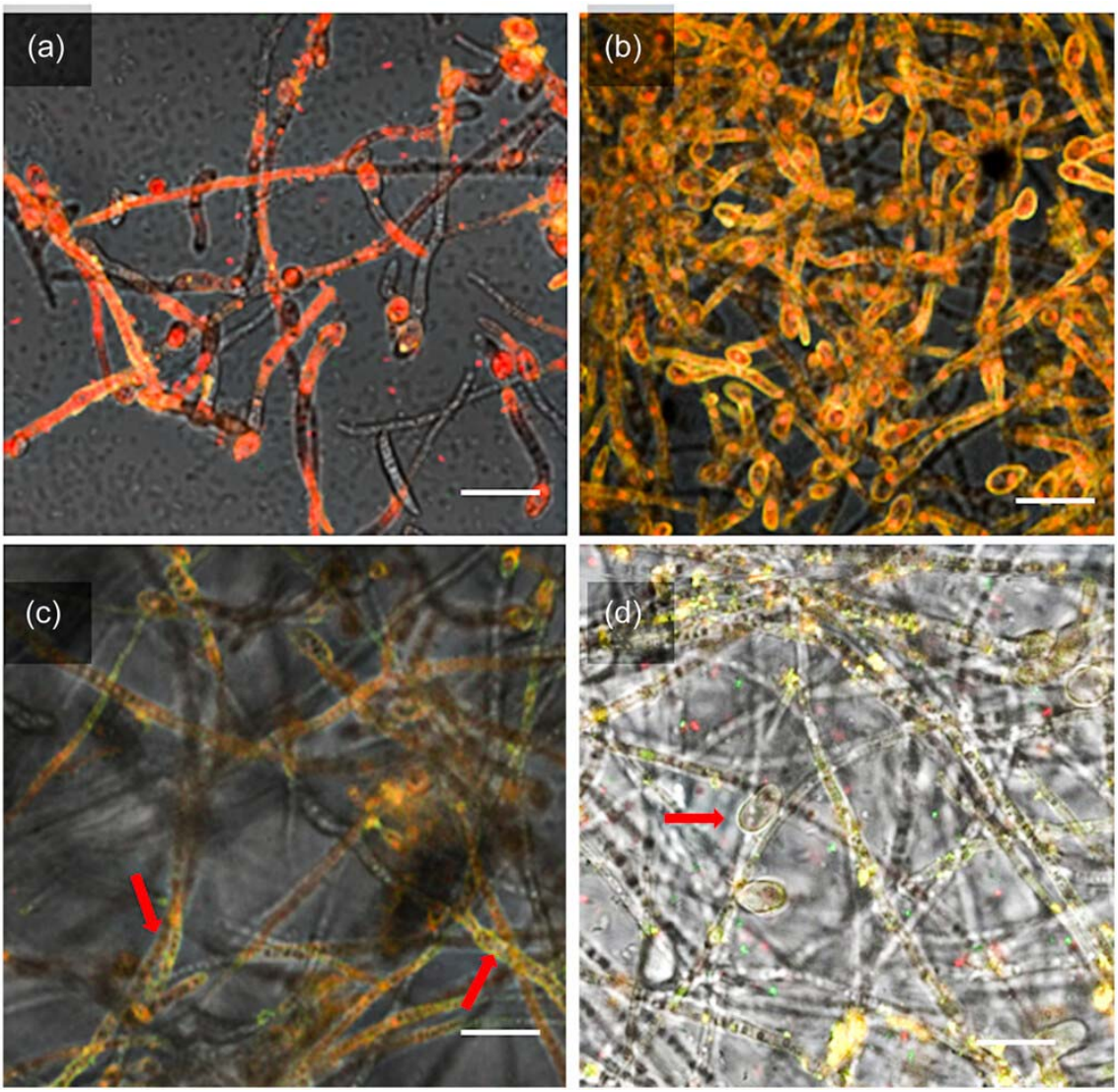

Figure 1. Confocal laser scanning microscopic imaging of *Fusarium circinatum* biofilms following growth in ¼ potato dextrose broth (PDB). The fluorescence cell wall polysaccharide-binding A-Alexa Fluor 488 conjugate (green) and the metabolically active cell binding Fun 1 (red). *F. circinatum* biofilms were dually stained over time. The different phases of biofilm formation of the FSP34 isolate were observed including (a, b) adhesion and microconidia phase, spores exhibiting metabolic activities (red-orange), (c, d) maturation and dispersal phase exhibiting extracellular polymeric matrix (ECM, yellow-green) production and dispersal of conidia (white arrow). The scale bar represents 10 µm.

3 RESULTS

3.1 *Fusarium circinatum* undergoes biofilm formation

Static incubation of *F. circinatum* in a Petri dish containing PDB produced biofilm-like structures (Figure S1). These closely resembled a pellicle, a type of biofilm that forms at the air–liquid interface of a liquid medium. Confocal laser scanning microscopy was used to observe over a period of 7 days the ability of the isolate to form biofilms. FUN1 was used to stain metabolically active cells red, and CAAF's green fluorescence was used to observe ECM

(Figure 1). After 24 h of incubation, the culture exhibited a red-fluorescing, aggregate of actively germinating conidia (Figure 1a). At 48 h, the culture was characterized by microcolony formation with pronounced hyphal growth and exhibited a yellowish fluorescence (combination of both FUN1 and CAAF stains) suggestive of the secretion of ECM (Figure 1b). At 72 h, the culture showed compacted hyphal networks stuck together by secreted ECM (Figure 1c). At 7 days, hyphal bundles seemed embedded in the ECM (largely stained by the CAAF stain) with some released conidial cells (Figure 1d). We thus regarded the 72-h culture as being a mature biofilm (early matured), while the 7-day-old (lately matured) culture represented a biofilm in its dispersal stage.

3.2 Stress is a distinguishing factor between biofilms and planktonic cells

According to SEM imaging analysis, *F. circinatum* FSP34 isolate forms dense and tightly packed mass of mycelial mat with innumerable interconnected hyphae (Figure 2a). SEM images further revealed the presence of inner channels interwoven like a trap. However, the ECM associated with biofilm formation was not apparent in the images, which could be attributed to the sample preparation process. We hypothesized that the reason for not observing ECM is that biofilms typically develop in response to stress conditions, which explains their recalcitrance to extreme environments [8]. Correspondingly, we observed that the ECM was not detectable under microscopic examination when the biofilm was incubated without any stress condition (Figure 2a). Due to this lack of observable ECM, the biofilm could not be distinguished from planktonic cells, as seen in Figure 2b, suggesting that a fully fledged biofilm is likely formed in the presence of some type of stress. Although this was the case, according to crystal violet staining (for cell wall components) and basic fuchsin staining (for nuclei and cytoplasmic granules), the amount of both biomass and ECM was more in biofilms than in planktonic cells although not significant (Figure 2b). To investigate whether stress can indeed induce a biofilm more defined in terms of these two traits, we subjected already grown biofilms to heat-shock treatment at 45°C, upon which the ECM and biomass were found to be significantly produced within 30–60 min of heat treatment in comparison to the control groups (Figure 2c,d). Furthermore, in comparison to Figure 2a, where we previously saw no ECM as there was no stress introduced, the ECM became more visible within 30–60 min of heat treatment, taking on the appearance of a cohesive adhesive substance that firmly secured the hyphae in place, as depicted in Figure 2c. This observation aligns very well with the expected role of ECM [42] and with previous reports on the physical appearance of ECM in filamentous plant fungal biofilms viewed under SEM [16, 24]. Furthermore, the research finding strongly suggests that the *F. circinatum* FSP34 biofilm undergoes a response mediated by the ECM and biomass (Figure 2d). Conversely, when compared to biofilms, planktonic cells displayed a markedly higher susceptibility to heat treatment. This heightened susceptibility was evident through a notable reduction in their metabolic activity compared to the control sample (Figure 2e; $p = 0.000001$), as measured by XTT, in contrast to the relatively more resilient metabolic activity observed in biofilms. This phenomenon is likely due to their cultivation under the influence of shear force caused by shaking, which may have prevented the sufficient production of ECM that often protects the biofilm [43]. The separate analysis of biomass (Figure 3a) and ECM (Figure 3b) reaffirmed the observation that heat treatment induces more robust biofilms in *F. circinatum*, with both characteristics significantly heightened compared to the control groups. Taken together, our findings clearly indicate fundamental differences in the general biology of planktonic cells and biofilms. They also strongly suggest that *F. circinatum* benefits from emergent properties provided by the biofilm traits (biomass and ECM) and is thus capable of forming true biofilms when confronted with stress.

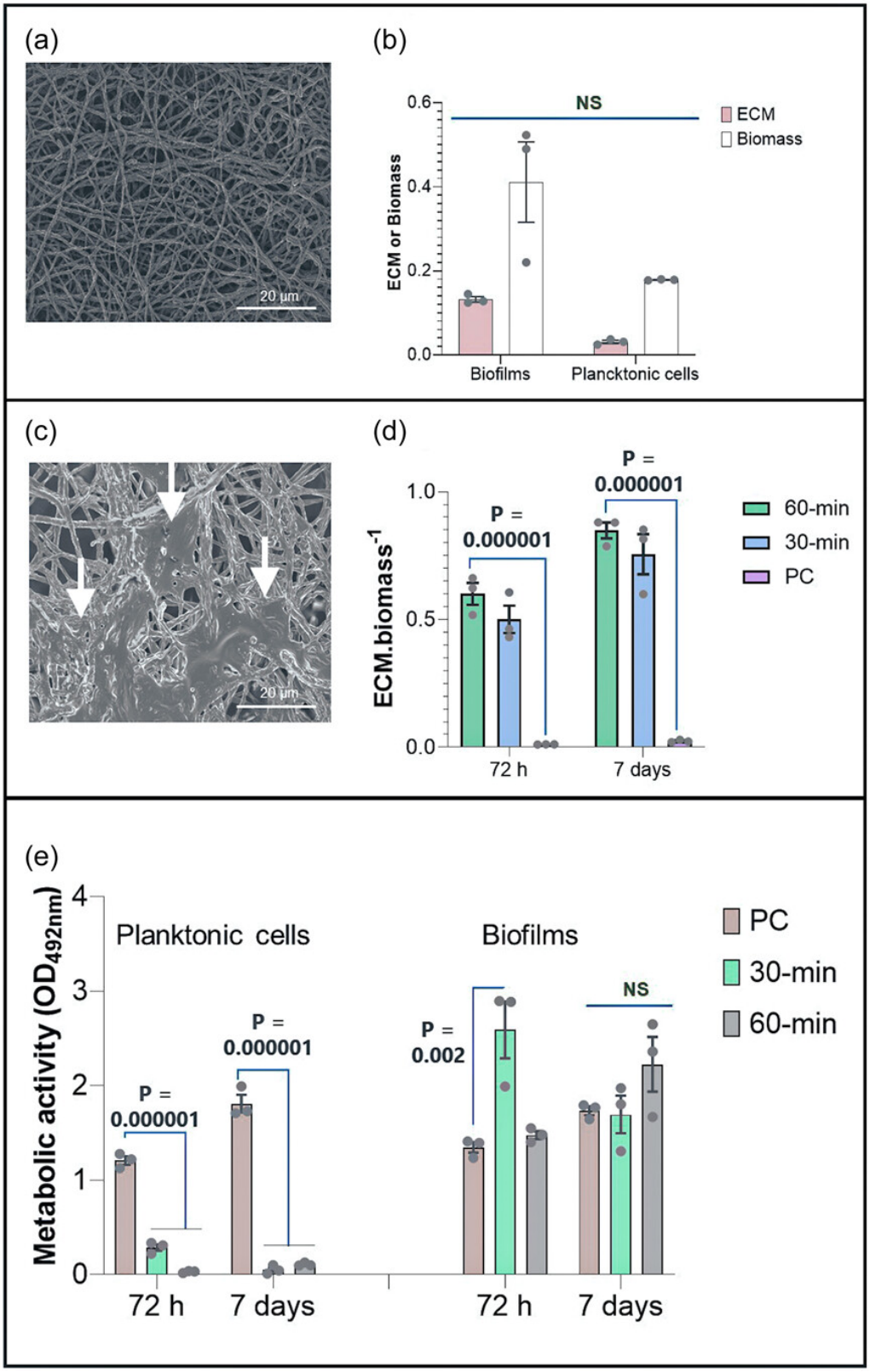

Figure 2. Effects of heat-shock (45°C for 30 and 60 min) on *Fusarium circinatum* planktonic cells and preformed biofilms. Growth in the absence (a, b) and presence (c, d) of heat. (a) A complex aggregated growth of hyphal bundles after 7 days at room temperature. (b) Planktonic cells and biofilms were

quantified in terms of extracellular matrix (ECM, at OD530 nm) produced and biomass (biomass at OD540 nm) at Day 7 following incubation. (c) Hyphae embedded in a secreted extracellular matrix (ECM) (white arrows) following heat shock. (d) ECM produced following heat shock lasting for an hour. (e) Effects on the metabolic activity (measured by 2,3-bis(2-methoxy-4-nitro-5-sulfophenyl)-2H-tetrazolium-5-carboxanilide reduction, recorded at an optical density of 492 nm) of planktonic cells and preformed biofilms. The means that were statistically different between samples using either student *t*-test or one-way analysis of variance were assigned a *p*-value ($p < 0.01$) while those lacking significant differences were indicated with "NS." Error bars indicate standard errors. $n = 3$, PC, positive control.

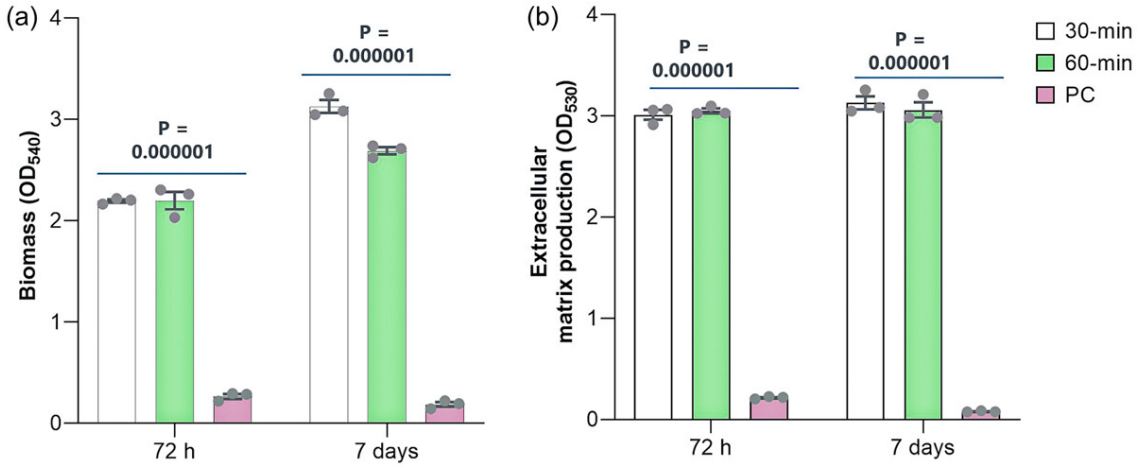

Figure 3. Effects of heat-shock (45°C for 30 and 60 min) on *Fusarium circinatum* preformed biofilms. Biofilm biomass (a) and extracellular matrix (ECM) produced (b) following heat-shock lasting for an hour. The means that were statistically different between samples were assigned a *p*-value ($p < 0.01$) while those lacking significant differences were indicated with "NS." Statistically different means between samples were analyzed using one-way analysis of variance and were assigned a *p*-value ($p < 0.01$) while those lacking significant differences were indicated with "NS." Error bars indicate standard errors. $n = 3$, PC, positive control.

3.3 *Fusarium circinatum* forms biofilms in the presence of abiotic factors

The effect of pH, temperature, sugars, and osmotic stresses on the ability of the FSP34 isolate to form a biofilm was measured in terms of metabolic activity using the XTT reduction assay at two time points (72 h and 7 days), as illustrated in Figure 4. In this assay, high optical density (OD) indicates an increase in the amount of metabolically active cells, which corresponds to either firmly attached biofilms (maximal ODs) or less firmly attached biofilms (suboptimal ODs). Overall optimal biofilm growth was observed at pH 6 at both time periods (Figure 4a). At the acidic conditions (pH 2, 3, and 4) less biofilm growth was observed, and under alkaline conditions (pH 8) the conidia used as inoculum failed to germinate (Figure 4a). Highest biofilm production was observed at 25°C and 30°C, with little to no metabolic activity observed at 4, 15, and 37°C in 72-h-old biofilms (Figure 4b). Increased metabolic activity and biofilm formation was observed on Day 7 at 15, 25, and 30°C, while low metabolic activity and biofilm formation was seen at 4°C and 37°C (Figure 4b). High metabolic activity was observed on Day 7 in the presence of glucose, lactose, and maltose, indicating strong biofilm formation (Figure 4c). Under osmotic stress conditions, biofilms developed in the presence of NaCl and sorbitol (Figure 4d), with increased metabolic activity observed after 72 h in NaCl compared to sorbitol. Metabolic activity decreased significantly at Day 7 under NaCl stress (Figure 4d).

We also took into account the ratio of ECM to cellular biomass (ECM.biomass^{-1}), which highlights the potential distribution of ECM components (polysaccharides, proteins, and nucleic acids) within the cells in a biofilm. The results showed a fluctuation of ECM production under subjected conditions, at which most exhibited insignificant statistical differences compared to the positive control (Figure S2A–D). This is an indication that during biofilm formation the ECM production per cell may not be prominently influenced by these conditions. Looking at biofilm traits (biomass and ECM) independently, however, revealed intriguing patterns in terms of response to both pH and temperature conditions (Figure 5). The data showed that the production of both biomass and ECM are greatly supported at pH 4 (Figure 5a,b) and under cold shock (4°C) (Figure 5c,d), respectively. A similar response that is based on heightened production of both these traits was observed previously (Figures 2 and 3), suggesting that under certain extreme conditions *F. circinatum* may form biofilms without trade-offs that is, biomass production over ECM and vice versa. However, there were no statistically significant differences observed in terms of ECM and biomass when the biofilm was cultured under the different sugars (Figure S3A,B). Likewise, under osmotic challenge the biofilm seemed unaffected (Figure 6a) except during exposure to 1 M NaCl, which resulted in significant production of ECM (Figure 6b). Unlike the pattern we observed under extreme heat (45°C) and cold (4°C) as well as low pH (4) where there was response in terms of both biomass and ECM, *F. circinatum* biofilms underwent ECM-mediated response when challenged with 1 M NaCl (Figure 6b).

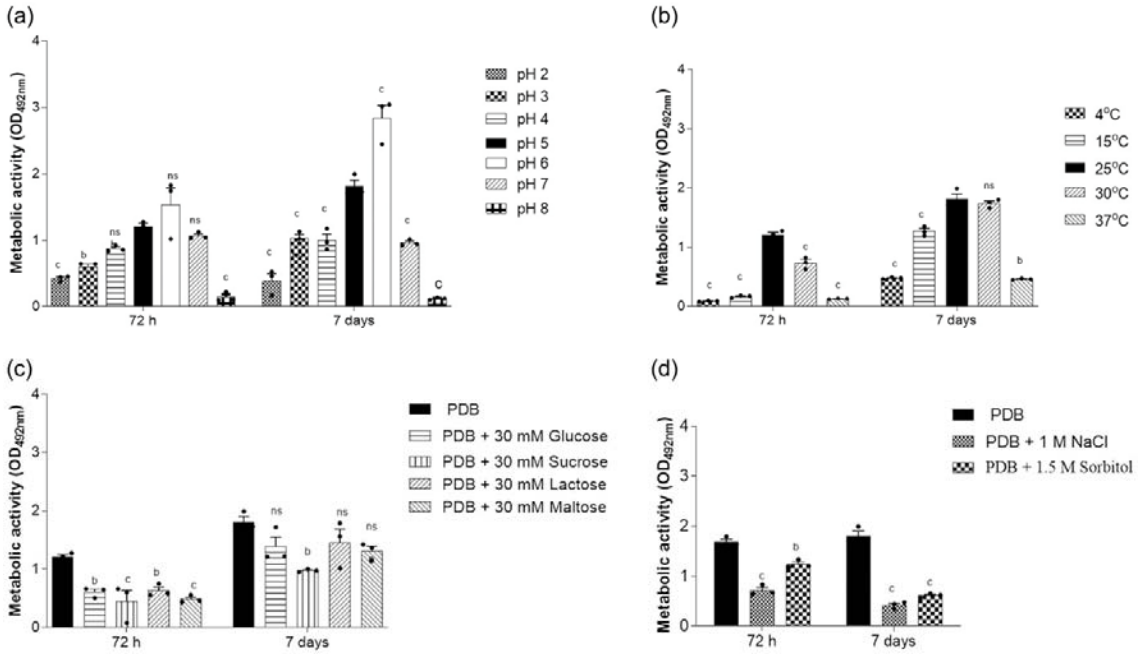

Figure 4. *Fusarium circinatum* biofilm formation in the presence of various pH conditions (a), carbon sources (b), osmotic stress (c), and temperature (d). The formation of biofilms was assessed for metabolic activity using 72-h and 7-day-old biofilms grown under various conditions (see text for detail on the growth media). The *y*-axis reflects metabolic activity as inferred using the 2,3-bis(2-methoxy-4-nitro-5-sulfophenyl)-2H-tetrazolium-5-carboxanilide (XTT) reduction assay. The XTT reduction was recorded at an optical density of 492 nm. Means that were statistically different ($p < 0.01$, one-way analysis of variance) between the various treatments at a particular time point are indicated with different letters, while those lacking significant differences were indicated with "abc". Error bars indicate standard errors. $n = 3$, PDB, potato dextrose broth.

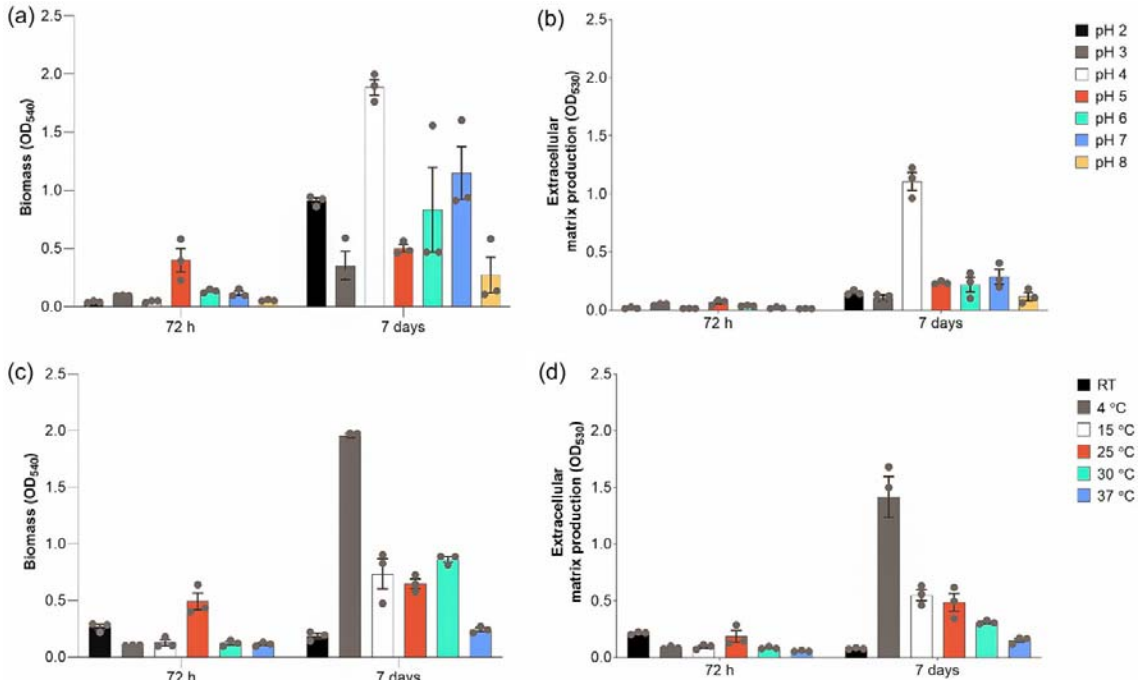

Figure 5. *Fusarium circinatum* biofilm formation influenced by pH (a, b) and temperature (c, d). The formation of biofilms was assessed using crystal violet for biomass and basic fuchsin for extracellular matrix (ECM) using 72 h and 7-day-old biofilms grown under various pH and temperature conditions (see text for detail on the growth media). PDB, potato dextrose broth, RT, room temperature.

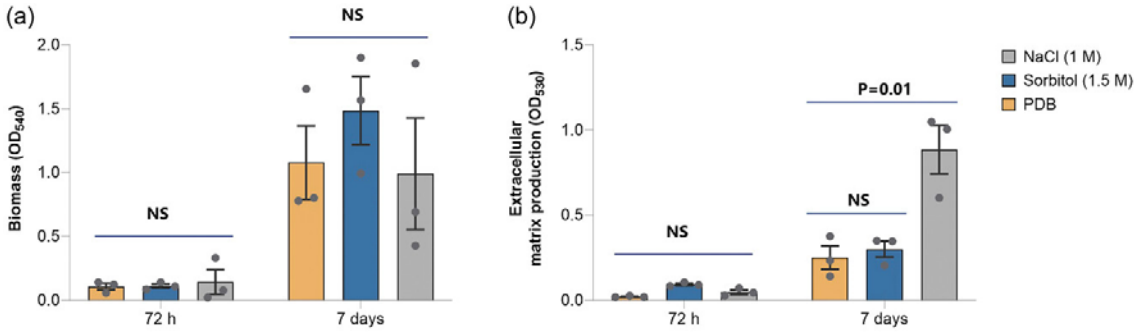

Figure 6. *Fusarium circinatum* biofilm formation under osmotic stress, measure in terms of biomass (a) and extracellular matrix (ECM) (b). The formation of biofilms was assessed using crystal violet for biomass and basic fuchsin for ECM using 72-h and 7-day-old biofilms. The means that were statistically different between samples were analyzed using a student *t*-test and assigned a *p*-value ($p < 0.01$) while those lacking significant differences were indicated with "NS." Error bars indicate standard errors. $n = 3$, PDB, potato dextrose broth.

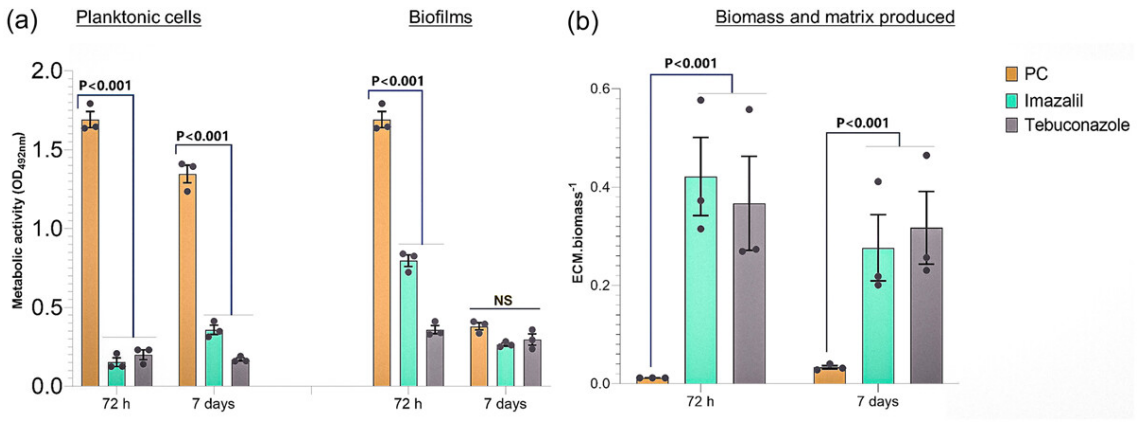

Figure 7. Comparison of metabolic activity for *Fusarium circinatum* biofilm and planktonic cultures after treatments with azole fungicides (a) and the extracellular matrix to biomass ratio for the biofilm (b). For these treatments, imazalil and tebuconazole were applied at their respective i50 concentrations to 72-h and 7-day-old biofilm and planktonic cultures. The means that were statistically different between the biofilm and planktonic culture, while those statistically different between treatments are assigned a p value ($p < 0.01$, one-way analysis of variance) while those lacking significant differences were indicated with "NS." Error bars indicate standard errors. $n = 3$, PC, positive control.

3.4 *F. circinatum* biofilms are potentially resistant to azoles

During the analysis of azole effects on mature biofilms, we first compared the general response of planktonic and biofilms to imazalil and tebuconazole. We first evaluated metabolic activity and ECM production per unit of biofilm biomass. The metabolic activity of the biofilms as well as the ECM produced was determined using identified I_{50} values (Table S1), in the presence of imazalil (750 µg/L) and tebuconazole (460 µg/L). The biofilm cells displayed high metabolic activity under azole treatment alone when compared to the untreated controls, particularly at 7 days (Figure 7a). Additionally, the biofilm metabolic response was accompanied by a significant increase in ECM per biomass, which was not seen in the untreated control samples (Figure 7b), in the presence of both azoles and at both 72 h and 7 days. Based on this result, biofilm cells appear to release substantial amounts of ECM per biomass in response to antifungals. This explains why the I_{50} values for both azoles are greater than those for planktonic cells and suggests that the tested azoles may be less effective antifungal agents on biofilms (Table S1). When we evaluated the production of ECM and biomass separately, we found biomass to be significantly inhibited only when the biofilm was exposed to Imazalil (Figure 8a). In contrast, in all other instances, no inhibition was observed (Figure 8b–d). ECM production was instead enhanced in treated samples compared to the controls, although only marginally (Figure 8b,d). This observation reinforces the hypothesis of potential resistance to azoles by *F. circinatum* biofilms.

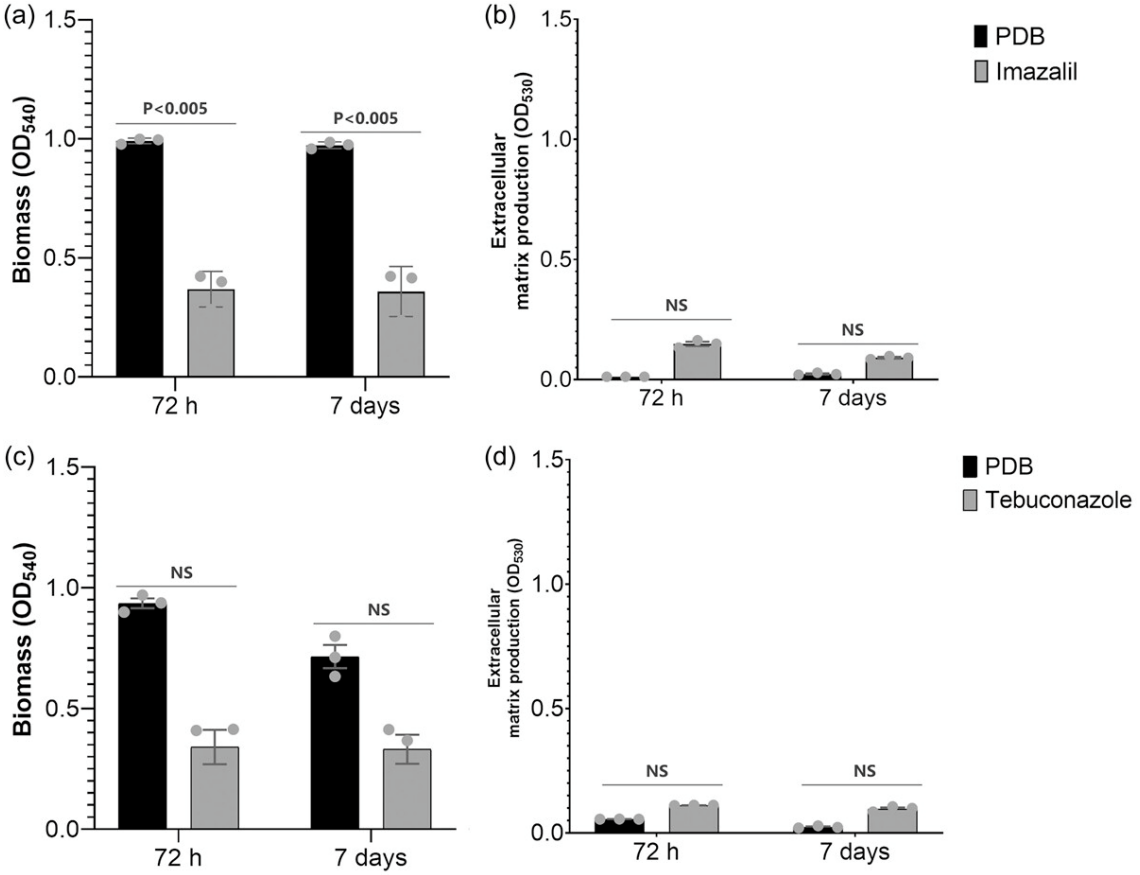

Figure 8. Biofilm response in terms of biomass and extracellular matrix (ECM) production toward imazalil and tebuconazole. For these treatments, imazalil, and tebuconazole were applied at their respective I_{50} concentrations (see text for details) to 72-h and 7-day-old biofilm. The impact of Imazalil on biomass (a) and ECM production (b). The impact of Tebucanozaole on biomass (c) and ECM production (d). The means that were statistically different are assigned a *p*-value ($p < 0.005$, one-way analysis of variance) while those lacking significant differences were indicated with "NS." Error bars indicate standard errors. $n = 3$, PDB, potato dextrose broth.

3.5 Azoles may interfere with DNase activity by increasing biofilm ECM levels

Exogenous application of DNase I is known to reduce early biofilm development and tolerance to antimicrobials by digesting eDNA, an essential biofilm structural component [44, 45]. To investigate this possibility, we first verified (Figure 9a,b) that the use of DNase I did, in fact, impact the integrity of biofilms as expected [38, 46]. Treatment of the 72-h and 7-day-old biofilms with DNase I did not seem to greatly impact their metabolic activity since the treated and untreated samples were not significantly different from one another (Figure 9a). This pattern changed when we used DNase + fungicide to treat the 72-h and 7-day-old biofilms. High metabolic activity was obtained for the azole+DNase I treatments of the 72-h biofilm (Figure 9a), as well as corresponding high ECM to biomass ratios (Figure 9b). Interestingly, metabolic activity remained higher in the $DNase^+$ samples (Figure 9a). Higher ECM levels were detected in the 72-h biofilms treated with DNase I and azole+DNase I, suggesting that DNase I can more easily destruct the younger *F. circinatum* biofilm. ECM levels were noticeably higher in the azole treatments (Figure 9b). For the 7-day-old biofilm we observed that the presence of azole+DNase I showed less impact on older biofilms, implying that the

fungicides may also not be able to penetrate through the biofilm. These results imply that azoles are a strong inducer of ECM production during all growth phases and will likely contribute to the eDNA's capability to maintain the integrity of the biofilm [47]. We observed no significant differences when biomass and ECM were analyzed individually (data not shown).

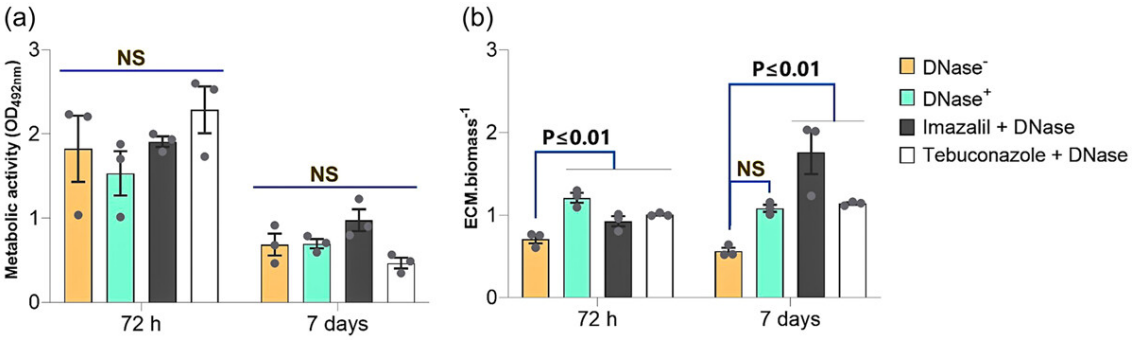

Figure 9. The metabolic effects of DNase I treatment on preformed biofilms with or without DNase or azole (a) and (b) corresponding extracellular matrix biomass-1 production. DNase, negative control. Means that were statistically different between the treatments are assigned a *p*-value ($p < 0.01$, one-way analysis of variance) while those lacking significant differences were indicated with "NS." Error bars indicate standard errors. $n = 3$.

4 DISCUSSION

We demonstrate here for the first time that *F. circinatum* forms biofilms under laboratory conditions. In this study, we detected the sequence of events involved in this biofilm formation (e.g., [18, 48-50]). Fluorescent dyes and light microscopy allowed observation of microcolony development in liquid culture and subsequent growth of biofilms characterized by ECM and tightly packed hyphae that formed conidia for subsequent dispersal. SEM studies provided evidence that tightly packed, homogenous mycelial mats were formed by interwoven hyphae which were "glued" together by ECM in forming such mats [24, 50]. Compared to planktonic cultures of *F. circinatum*, the biofilms were also substantially more metabolically active and displayed distinct properties. The biofilms produced by *F. circinatum* are comparable to true biofilms reported for *Aspergillus*, *Fusarium*, *Botrytis*, and *Verticillium* species [17, 18, 24, 25, 38, 51].

As a life history trait, the ability to form biofilms could have far-reaching implications for our understanding of the biology of *F. circinatum*. This is because biofilms afford physical protection from environmental change, while also allowing dynamic responses to cope with stress and to exploit resources at their disposal [50, 52]. As have been shown for bacterial pathogens of vascular plants [53], biofilm formation might contribute to the ability of *F. circinatum* to overcome the defense mechanisms employed by its conifer host [25, 54]. The fungus colonizes pine, first by spreading laterally along the xylem and then into the pith and cortex where it sporulates [55-57]. During the process, *F. circinatum* preferentially targets xylem-associated resin ducts and their formation, in doing so exploiting for its own benefit one of the plant's primary defenses against pathogen attack [55]. The fact that this pathogen can also develop a floating type of biofilms (pellicles), suggests that it can easily travel within the plant vasculature as microcolonies while being protected by the ECM from plant surveillance as observed with other pathogens that can spread conidia within the different parts of a host [58]. Future research should therefore investigate whether biofilm formation is needed for

colonizing plant tissues, particularly resin ducts, and whether ECM polymers such as EPS and eDNA are needed for pathogenesis.

Our results suggest that biofilm formation may benefit *F. circinatum* across a diverse range of environmental conditions. Biofilm formation was highest under neutral conditions whereby the fungus retained the ability even at slightly more acidic conditions, which corresponds with the pH range (3.3–6.4) found in the pine tissues it colonizes [59]. In particular, the observation that biomass and ECM production are optimum at pH 4 further supports this conclusion. Various sugars also supported the biofilm formation, which is consistent with the range of polysaccharides the fungus might encounter in the plant environment, either as part of the plants storage molecules or those produced by the fungus when it degrades the plant's cell walls e.g [60, 61]. Biofilms might also support various other ecological activities that have been suggested for *F. circinatum* [61, 62]. For instance, either pellicle biofilm formation may influence long distance disease spread or climate change may cause release of highly resistant persister cells due to disruption of the biofilm structures [8, 63-65]. Additionally, *F. circinatum* would likely retain the benefits of biofilm formation outside the plant host, as this growth form was supported at different osmotic stresses and in a range of temperatures. Although the fungus does not grow at ≤5°C and ≥40°C when grown conventionally on agar medium [66, 67], we observed biofilm formation at temperatures ranging from 4°C to 37°C, with 4°C supporting both biomass and ECM production at optimal levels than any other temperature. As seen in yeast, we speculate that the biofilm, especially the ECM, can serve to protect the fungus from extreme conditions such as low pH and temperature, even if it just to enable survival until conditions are more favorable [68-70].

Biofilms and planktonic cultures of *F. circinatum* were distinctive in their response to the agricultural azole fungicides imazalil and tebuconazole. Both these agents target ergosterol biosynthesis by inhibiting the activity of the cytochrome P450 enzyme, ergosterol 14-α-demethylase (CYP51/ERG11) and are known for their efficacy against various *Fusarium* [71-74]. As expected [18], planktonic cultures of *F. circinatum* were much susceptible to these fungicides than the biofilm cultures. A level of 50% growth inhibition required much less of the fungicide in the planktonic cultures (i.e., 0.04 mg/L tebuconazole and 0.26 mg/L imazalil) than in the biofilm cultures (i.e., 0.46 mg/L tebuconazole and 0.74 mg/L imazalil). In other microorganisms, such resistance to azoles may be mediated by various factors, including ECM production [75-77]. Indeed, more ECM was produced per cell biomass by *F. circinatum* in the presence of these two azoles, which likely acted as a barricade against diffusion into the interior of the biofilm [41]. However, this effect seemed to decrease over time, as fungicides caused a reduction in the metabolic activity and biomass from 72 h to Day 7. The older biofilms were likely made up of dormant, dying, or dead cells, which might serve as a nutrient source for actively growing cells [78]. It would thus be interesting to investigate biofilm formation and maintenance over longer time periods.

Our data showed that eDNA is a crucial aspect of *F. circinatum* biofilms, particularly when the fungus is challenged with fungicides. DNase I treatment of pre-formed biofilms substantially reduced their metabolic activity, but caused increased in the production of ECM irrespective of whether a fungicide treatment was applied or not. Although not investigated in this study, previous studies have shown that DNase is expected to have high antibiofilm efficiency during early biofilm formation because immature biofilms have a less complex architecture, with very little ECM [45, 79]. This could mean improved penetration of the biofilm when it contains less eDNA, but the latter presents a stress or trigger that increases ECM production. In the case of imazalil+DNase I, the treatment enhanced ECM production and metabolic activity of 7-day-

old biofilms to levels higher than those observed for the no-DNase control. Such an improvement by DNase I in the efficacy of fungicides is also known from other fungi [46].

Apart from showing that fungicide application might have effects opposite to what was expected (e.g., improved azole efficacy), our data complements the growing body of information regarding the importance of eDNA for plant pathogens. Although most environments are rich in eDNA and extracellular DNases [80, 81], these two elements can also be exploited by interacting organisms during their arms race. For example, in the biofilm environment certain bacteria parasitize fungi using Mg^{2+}-dependent DNase for degrading the fungal DNA [82, 83]. During the interaction between maize and the fungal pathogen *Cochliobolus heterostrophus*, plant produced eDNA is crucial for plant immunity (i.e., DNase I enhances the pathogen's virulence) [84]. Taken together, we posit that eDNA is a common occurrence in the life of *F. circinatum* and that it has relevant mechanisms for combatting such "DNase stress" as seen through increased ECM production, irrespective of the source of the nuclease. In the current study, this was in the form of increased ECM production and enhanced metabolic activity. It would be interesting to further explore this hypothesis and to determine whether eDNA also plays a role during planktonic growth of the fungus.

Besides improving our understanding of the biology of *F. circinatum*, the results of this study have implications with regard to the management strategies employed in the control of this fungus in the seedling and plantation environment. It is reasonable to suggest that *F. circinatum* can also establish biofilms in and on various abiotic substrates and surfaces encountered in pine seedling nurseries and plantations. Although various control strategies are typically employed for controlling *F. circinatum*-associated disease [22, 85] it is unknown how biofilm formation might influence their efficacy. Also, even if they prove effective on biofilms, large-scale applications might not always reach the desired treatment levels (e.g., temperatures or fungicide concentrations). Such control failures might thus stimulate enhanced growth and inoculum production. This is abundantly illustrated in our study, where treatment at 45°C (a temperature thought to inhibit the fungus) increased the metabolic activity, biomass, and ECM production to levels substantially higher than those recorded in the absence of the heat treatment. Therefore, the efficacy of the standard control measures requires re-evaluation under this new paradigm of biofilm formation being part of the life history traits of *F. circinatum*.

AUTHOR CONTRIBUTIONS

Francinah M. Ratsoma: Conceptualization; formal analysis; investigation; methodology; validation; visualization; writing—original draft; writing—review and editing. **Nthabiseng Z. Mokoena**: Investigation; methodology; validation; writing—review and editing. **Quentin C. Santana**: Project administration; supervision; writing—review and editing. **Brenda D. Wingfield**: Project administration; resources; supervision; writing—original draft; writing—review and editing. **Emma T. Steenkamp**: Project administration; resources; supervision; writing—original draft; writing—review and editing. **Thabiso E. Motaung**: Conceptualization; formal analysis; funding acquisition; investigation; methodology; project administration; resources; supervision; writing—original draft; writing—review and editing.

ACKNOWLEDGMENTS

The work was funded by Thuthuka funding instrument (Grant No. 129580) of the South African National Research Foundation (NRF), and the South African National Department of

Science and Innovation-NRF Centers of Excellence program and South African Research Chairs Initiative (Grant No. 98353).

CONFLICT OF INTEREST STATEMENT

The authors declare no conflict of interest.

REFERENCES

1. Mitchell KF, Zarnowski R, Andes DR. Fungal super glue: the biofilm matrix and its composition, assembly, and functions. *PLoS Pathog*. 2016; 12:e1005828.
2. Sheppard DC, Howell PL. Biofilm exopolysaccharides of pathogenic fungi: lessons from bacteria. *J Biol Chem*. 2016; 291: 12529–12537.
3. Flemming HC, Wingender J. The biofilm matrix. *Nat Rev Microbiol*. 2010; 8: 623–633.
4. HC Flemming, TR Neu, J Wingender, editors. The perfect slime: Microbial extracellular polymeric substances (EPS). London: IWA Publishing; 2016.
5. Beauvais A, Schmidt C, Guadagnini S, Roux P, Perret E, Henry C, et al. An extracellular matrix glues together the aerial-grown hyphae of *Aspergillus fumigatus*. *Cell Microbiol*. 2007; 9: 1588–1600.
6. Karygianni L, Paqué PN, Attin T, Thurnheer T. Single DNase or proteinase treatment induces change in composition and structural integrity of multispecies oral biofilms. *Antibiotics*. 2021; 10: 400.
7. Harding MW, Marques LL, Shore B, Daniels GC. The significance of fungal biofilms in association with plants and soils. In: I Ahmad, FM Husain, editors. Biofilms in Plant and Soil Health. Chichester, UK: John Wiley & Sons; 2017. p. 131–149.
8. Motaung TE, Peremore C, Wingfield B, Steenkamp E. Plant-associated fungal biofilms—knowns and unknowns. *FEMS Microbiol Ecol*. 2020; 96:fiaa224.
9. Costerton JW, Cheng KJ, Geesey GG, Ladd TI, Nickel JC, Dasgupta M, et al. Bacterial biofilms in nature and disease. *Annu Rev Microbiol*. 1987; 41: 435–464.
10. Costerton J. Introduction to biofilm. *Int J Antimicro Ag*. 1999; 11: 217–221.
11. McDougald D, Rice SA, Barraud N, Steinberg PD, Kjelleberg S. Should we stay or should we go: mechanisms and ecological consequences for biofilm dispersal. *Nat Rev Microbiol*. 2012; 10: 39–50.
12. Harding M, Nadworny P, Buziak B, Omar A, Daniels G, Feng J. Improved methods for treatment of phytopathogenic biofilms: metallic compounds as anti-bacterial coatings and fungicide 1tank-mix partners. *Molecules*. 2019; 24: 2312.
13. Marques LLR, Ceri H, Manfio GP, Reid DM, Olson ME. Characterization of biofilm formation by *Xylella fastidiosa* in vitro. *Plant Dis*. 2002; 86: 633–638.
14. Lowe-Power TM, Khokhani D, Allen C. How *Ralstonia solanacearum* exploits and thrives in the flowing plant xylem environment. *TIM*. 2018; 26: 929–942.
15. Abdel-Aziz MM, Emam TM, Elsherbiny EA. Effects of mandarin (*Citrus reticulata*) peel essential oil as a natural antibiofilm agent against *Aspergillus niger* in onion bulbs. *Postharvest Biol Technol*. 2019; 156:110959.
16. Tyzack TE, Hacker C, Thomas G, Fones HN. Biofilm formation in *Zymoseptoria tritici*. *bioRxiv*. 2023. https://doi.org/10.1101/2023.07.26.550639
17. Harding MW, Marques LL, Howard RJ, Olson ME. Biofilm morphologies of plant pathogenic fungi. *Am J Plant Sci Biotechnol*. 2010; 4: 43–47.
18. Peiqian L, Xiaoming P, Huifang S, Jingxin Z, Ning H, Birun L. Biofilm formation by *Fusarium oxysporum f. sp. cucumerinum* and susceptibility to environmental stress. *FEMS Microbiol Lett*. 2014; 350: 138–145.
19. Martínez-Álvarez P, Pando V, Diez JJ. Alternative species to replace Monterey pine plantations affected by pitch canker caused by *Fusarium circinatum* in northern Spain. *Plant Pathol*. 2014; 63: 1086–1094.

20. Martín-García J, Lukačevičová A, Flores-Pacheco J, Diez J, Dvořák M. Evaluation of the susceptibility of several Czech conifer provenances to *Fusarium circinatum*. *Forests*. 2018; 9: 72.
21. Wingfield MJ, Hammerbacher A, Ganley RJ, Steenkamp ET, Gordon TR, Wingfield BD, et al. Pitch canker caused by *Fusarium circinatum*—a growing threat to pine plantations and forests worldwide. *Austr Plant Pathol*. 2008; 37: 319–334.
22. Zamora-Ballesteros C, Diez JJ, Martín-García J, Witzell J, Solla A, Ahumada R, et al. Pine pitch canker (PPC): pathways of pathogen spread and preventive measures. *Forests*. 2019; 10: 1158.
23. Drenkhan R, Ganley B, Martín-García J, Vahalík P, Adamson K, Adamčíková K, et al. Global geographic distribution and host range of *Fusarium circinatum*, the causal agent of pine pitch canker. *Forests*. 2020; 11: 724.
24. Peremore C, Wingfield B, Santana Q, Steenkamp ET, Motaung TE. Biofilm characterization in the maize pathogen, *Fusarium verticillioides*. *bioRxiv*. 2022. https://doi.org/10.1101/2022.11.18.517162
25. Shay R, Wiegand AA, Trail F. Biofilm formation and structure in the filamentous fungus *Fusarium graminearum*, a plant pathogen. *Microbiol Spectr*. 2022; 10:e00171-22.
26. de Vos L, van der Nest MA, van der Merwe NA, Myburg AA, Wingfield MJ, Wingfield BD. Genetic analysis of growth, morphology and pathogenicity in the F1 progeny of an interspecific cross between *Fusarium circinatum* and *Fusarium subglutinans*. *Fungal Biol*. 2011; 115: 902–908.
27. Desjardins AE, Plattner RD, Gordon TR. *Gibberella fujikuroi* mating population A and *Fusarium subglutinans* from teosinte species and maize from Mexico and Central America. *Mycol Res*. 2000; 104: 865–872.
28. Swalarsk-Parry BS, Steenkamp ET, van Wyk S, Santana QC, van der Nest MA, Hammerbacher A, et al. Identification and characterization of a QTL for growth of *Fusarium circinatum* on pine-based medium. *J Fungi*. 2022; 8: 1214.
29. Phasha MM, Wingfield BD, Wingfield MJ, Coetzee MPA, Hammerbacher A, Steenkamp ET. Deciphering the effect of FUB1 disruption on fusaric acid production and pathogenicity in *Fusarium circinatum*. *Fungal Biol*. 2021; 125: 1036–1047.
30. Phasha MM, Wingfield MJ, Wingfield BD, Coetzee MPA, Hallen-Adams H, Fru F, et al. Ras2 is important for growth and pathogenicity in *Fusarium circinatum*. *Fungal Genet Biol*. 2021; 150:103541.
31. Mowat E, Butcher J, Lang S, Williams C, Ramage G. Development of a simple model for studying the effects of antifungal agents on multicellular communities of *Aspergillus fumigatus*. *J Med Microbiol*. 2007; 56: 1205–1212.
32. Ommen P, Zobek N, Meyer RL. Quantification of biofilm biomass by staining: non-toxic safranin can replace the popular crystal violet. *J Microbiol Meth*. 2017; 141: 87–89.
33. Peeters E, Nelis HJ, Coenye T. Comparison of multiple methods for quantification of microbial biofilms grown in microtiter plates. *J Microbiol Meth*. 2008; 72: 157–165.
34. Bhandari S, Khadayat K, Poudel S, Shrestha S, Shrestha R, Devkota P, et al. Phytochemical analysis of medicinal plants of Nepal and their antibacterial and antibiofilm activities against uropathogenic *Escherichia coli*. *BMC Complement Med Ther*. 2021; 21: 116.
35. Roehm NW, Rodgers GH, Hatfield SM, Glasebrook AL. An improved colorimetric assay for cell proliferation and viability utilizing the tetrazolium salt XTT. *J Immunol Methods*. 1991; 142: 257–265.
36. Choi NY, Kang SY, Kim KJ. *Artemisia princeps* inhibits biofilm formation and virulence-factor expression of antibiotic-resistant bacteria. *BioMed Res Int*. 2015; 2015: 1–7.
37. Peng D. Biofilm formation of *Salmonella*. In: Microbial biofilms-importance and applications. Janeza Trdine, Croatia: InTech; 2016. p. 231–242. https://doi.org/10.5772/62905
38. Rajendran R, Williams C, Lappin DF, Millington O, Martins M, Ramage G. Extracellular DNA release acts as an antifungal resistance mechanism in mature *Aspergillus fumigatus* biofilms. *Eukaryotic Cell*. 2013; 12: 420–429.

39. Rajendran R, Sherry L, Lappin DF, Nile CJ, Smith K, Williams C, et al. Extracellular DNA release confers heterogeneity in *Candida albicans* biofilm formation. *BMC Microbiol*. 2014; 14: 303.
40. Leggate J, Allain R, Isaac L, Blais BW. Microplate fluorescence assay for the quantification of double stranded DNA using SYBR Green I dye. *Biotechnol Lett*. 2006; 28: 1587–1594.
41. Ramage G, Rajendran R, Sherry L, Williams C. Fungal biofilm resistance. *Int J Microbiol*. 2012; 2012: 1–14.
42. 42Flemming HC, van Hullebusch ED, Neu TR, Nielsen PH, Seviour T, Stoodley P, et al. The biofilm matrix: multitasking in a shared space. *Nat Rev Microbiol*. 2023; 21: 70–86.
43. Hawser SP, Baillie GS, Douglas LJ. Production of extracellular matrix by *Candida albicans* biofilms. *J Med Microbiol*. 1998; 47: 253–256.
44. Whitchurch CB, Tolker-Nielsen T, Ragas PC, Mattick JS. Extracellular DNA required for bacterial biofilm formation. *Science*. 2002; 295: 1487.
45. Tetz GV, Artemenko NK, Tetz VV. Effect of DNase and antibiotics on biofilm characteristics. *Antimicrob Agents Chemother*. 2009; 53: 1204–1209.
46. Martins M, Henriques M, Lopez-Ribot JL, Oliveira R. Addition of DNase improves the in vitro activity of antifungal drugs against *Candida albicans* biofilms. *Mycoses*. 2012; 55: 80–85.
47. Martins M, Uppuluri P, Thomas DP, Cleary IA, Henriques M, Lopez-Ribot JL, et al. Presence of extracellular DNA in the *Candida albicans* biofilm matrix and its contribution to biofilms. *Mycopathologia*. 2010; 169: 323–331.
48. Chandra J, Mukherjee PK, Leidich SD, Faddoul FF, Hoyer LL, Douglas LJ, et al. Antifungal resistance of candidal biofilms formed on denture acrylic in vitro. *J Dent Res*. 2001; 80: 903–908.
49. Seidler MJ, Salvenmoser S, Müller FMC. *Aspergillus fumigatus* forms biofilms with reduced antifungal drug susceptibility on bronchial epithelial cells. *Antimicrob Agents Chemother*. 2008; 52: 4130–4136.
50. Harding MW, Marques LLR, Howard RJ, Olson ME. Can filamentous fungi form biofilms? *TIM*. 2009; 17: 475–480.
51. Siqueira VM, Lima N. Biofilm formation by filamentous fungi recovered from a water system. *J Mycol*. 2013; 2013: 1–9.
52. Pandit A, Adholeya A, Cahill D, Brau L, Kochar M. Microbial biofilms in nature: unlocking their potential for agricultural applications. *J Appl Microbiol*. 2020; 129: 199–211.
53. Mina IR, Jara NP, Criollo JE, Castillo JA. The critical role of biofilms in bacterial vascular plant pathogenesis. *Plant Pathol*. 2019; 68: 1439–1447.
54. Kolosova N, Bohlmann J Conifer defense against insects and fungal pathogens. In: R Matyssek, H Schnyder, W Oßwald, D Ernst, JC Munch, H Pretzsch, editors. Growth and defence in plants: resource allocation at multiple scales. Berlin Heidelberg: Springer; 2012. p. 85–109.
55. Martín-Rodrigues N, Espinel S, Sanchez-Zabala J, Ortíz A, González-Murua C, Duñabeitia MK. Spatial and temporal dynamics of the colonization of *Pinus* radiata by *Fusarium circinatum*, of conidiophora development in the pith and of traumatic resin duct formation. *New Phytol*. 2013; 198: 1215–1227.
56. Martín-Rodrigues N, Sanchez-Zabala J, Salcedo I, Majada J, González-Murua C, Duñabeitia MK. New insights into radiata pine seedling root infection by *Fusarium circinatum*. *Plant Pathol*. 2015; 64: 1336–1348.
57. Swett CL, Kirkpatrick SC, Gordon TR. Evidence for a hemibiotrophic association of the pitch canker pathogen *Fusarium circinatum* with *Pinus radiata*. *Plant Dis*. 2016; 100: 79–84.
58. Pietro AD, Madrid MP, Caracuel Z, Delgado-Jarana J, Roncero MIG. *Fusarium oxysporum*: exploring the molecular arsenal of a vascular wilt fungus. *Mol Plant Pathol*. 2003; 4: 315–325.
59. Geffert A, Geffertova J, Dudiak M. Direct method of measuring the pH value of wood. *Forests*. 2019; 10: 852.
60. Chimwamurombe PM, Wingfield BD, Botha AM, Wingfield MJ. Cloning and sequence analysis of the endopolygalacturonase gene from the pitch canker fungus, *Fusarium circinatum*. *Curr Microbiol*. 2001; 42: 350–352.
61. Seiboth B, Pakdaman BS, Hartl L, Kubicek CP. Lactose metabolism in filamentous fungi: how to deal with an unknown substrate. *Fungal Biol Rev*. 2007; 21: 42–48.

62. Gordon TR, Reynolds GJ. Plasticity in plant-microbe interactions: a perspective based on the pitch canker pathosystem. *Phytoparasitica*. 2017; 45: 1–8.
63. Garbelotto M, Smith T, Schweigkofler W. Variation in rates of spore deposition of *Fusarium circinatum*, the causal agent of pine pitch canker, over a 12-month-period at two locations in Northern California. *Phytopathology®*. 2008; 98: 137–143.
64. Martins PMM, Merfa MV, Takita MA, de Souza AA. Persistence in phytopathogenic bacteria: do we know enough? *Front Microbiol*. 2018; 9: 1099.
65. Gollan B, Grabe G, Michaux C, Helaine S. Bacterial persisters and infection: past, present, and progressing. *Annu Rev Microbiol*. 2019; 73: 359–385.
66. Mullett M, Pérez-Sierra A, Armengol J, Berbegal M. Phenotypical and molecular characterisation of *Fusarium circinatum*: correlation with virulence and fungicide sensitivity. *Forests*. 2017; 8: 458.
67. Elvira-Recuenco M, Pando V, Berbegal M, Manzano Muñoz A, Iturritxa E, Raposo R. Influence of temperature and moisture duration on pathogenic life history traits of predominant haplotypes of *Fusarium circinatum* on *Pinus* spp. *Phytopathology®*. 2021; 111: 2002–2009.
68. Moryl M, Kaleta A, Strzelecki K, Różalska S, Różalski A. Effect of nutrient and stress factors on polysaccharides synthesis in *Proteus mirabilis* biofilm. *Acta Biochim Pol*. 2014; 61: 133–139.
69. Pemmaraju SC, Padmapriya K, Pruthi PA, Prasad R, Pruthi V. Impact of oxidative and osmotic stresses on *Candida albicans* biofilm formation. *Biofouling*. 2016; 32: 897–909.
70. Villa F, Remelli W, Forlani F, Gambino M, Landini P, Cappitelli F. Effects of chronic sub-lethal oxidative stress on biofilm formation by *Azotobacter vinelandii*. *Biofouling*. 2012; 28: 823–833.
71. Audenaert K, Landschoot S, Vanheule A, Waegeman W, de Baets B, Haesaert G. Impact of fungicide timing on the composition of the *Fusarium* head blight disease complex and the presence of deoxynivalenol (DON) in wheat. In: M Thajuddin, editor. Fungicides-beneficial and harmful aspects. 16IntechOpen; 2011. p. 79–98.
72. Odds FC, Brown AJP, Gow NAR. Antifungal agents: mechanisms of action. *TIM*. 2003; 11: 272–279.
73. Berbegal M, Landeras E, Sánchez D, Abad-Campos P, Pérez-Sierra A, Armengol J. Evaluation of *Pinus radiata* seed treatments to control *Fusarium circinatum*: effects on seed emergence and disease incidence. *Forest Pathol*. 2015; 45: 525–533.
74. Tini F, Beccari G, Onofri A, Ciavatta E, Gardiner DM, Covarelli L. Fungicides may have differential efficacies towards the main causal agents of *Fusarium* head blight of wheat. *Pest Manag Sci*. 2020; 76: 3738–3748.
75. Kaur J, Nobile CJ. Antifungal drug-resistance mechanisms in *Candida biofilms*. *Curr Opin Microbiol*. 2023; 71:102237.
76. Nett JE, Crawford K, Marchillo K, Andes DR. Role of Fks1p and matrix glucan in *Candida albicans* biofilm resistance to an echinocandin, pyrimidine, and polyene. *Antimicrob Agents Chemother*. 2010; 54: 3505–3508.
77. Sardi JDCO, Pitangui NDS, Rodríguez-Arellanes G, Taylor ML, Fusco-Almeida AM, Mendes-Giannini MJS. Highlights in pathogenic fungal biofilms. *Revista Iberoamericana de Micología*. 2014; 31: 22–29.
78. Gilbert P, Maira-Litran T, McBain AJ, Rickard AH, Whyte FW. The physiology and collective recalcitrance of microbial biofilm communities. *Adv Microb Physiol*. 2002; 46: 203–256.
79. Schlafer S, Garcia J, Meyer RL, Vaeth M, Neuhaus KW. Effect of DNase treatment on adhesion and early biofilm formation of *Enterococcus faecalis*. *Eur Endod J*. 2018; 3: 82–86.
80. Foucher A, Evrard O, Ficetola GF, Gielly L, Poulain J, Giguet-Covex C, et al. Persistence of environmental DNA in cultivated soils: implication of this memory effect for reconstructing the dynamics of land use and cover changes. *Sci Rep*. 2020; 10:10502.
81. Yang K, Wang L, Cao X, Gu Z, Zhao G, Ran M, et al. The origin, function, distribution, quantification, and research advances of extracellular DNA. *Int J Mol Sci*. 2022; 23:13690.
82. Luo J, Chu X, Jie J, Sun Y, Guan Q, Li D, et al. *Acinetobacter baumannii* kills fungi via a type VI DNase effector. *mBio*. 2023; 14: e03420–e03422.

83. Park HJ, Wang W, Curlango-Rivera G, Xiong Z, Lin Z, Huskey DA, et al. A DNase from a fungal phytopathogen is a virulence factor likely deployed as counter defense against host-secreted extracellular DNA. *mBio*. 2019; 10: e02805–e02818.
84. Monticolo F, Palomba E, Termolino P, Chiaiese P, de Alteriis E, Mazzoleni S, et al. The role of DNA in the extracellular environment: a focus on NETs, RETs and biofilms. *Front Plant Sci*. 2020; 11:589837.
85. Iturritxa E, Trask T, Mesanza N, Raposo R, Elvira-Recuenco M, Patten C. Biocontrol of *Fusarium circinatum* infection of young *Pinus radiata* trees. *Forests*. 2017; 8: 32.